Understanding the influence of the bioaerosol source on the distribution of airborne bacteria in hospital indoor air

Víctor Pertegal[1], Engracia Lacasa[1]*, Pablo Cañizares[2], Manuel A. Rodrigo[2], Cristina Sáez[2]*

[1]Department of Chemical Engineering, Higher Technical School of Industrial Engineering, University of Castilla-La Mancha, Edificio Infante Don Juan Manuel, Campus Universitario s/n, 02071 Albacete, Spain

[2]Department of Chemical Engineering, Faculty of Chemical Sciences and Technologies, University of Castilla-La Mancha, Edificio Enrique Costa Novella, Campus Universitario s/n, 13005 Ciudad Real, Spain

*authors to whom all correspondence should be addressed (corresponding authors): engracia.lacasa@uclm.es; cristina.saez@uclm.es.

1

21   **Abstract**

22   The composition and concentration of airborne microorganisms in hospital indoor air has

23   been reported to contain airborne bacteria and fungi concentrations ranged $10^1 - 10^3$

24   CFU/m^3 in inpatients facilities which mostly exceed recommendations from the World

25   Health Organization (WHO). In this work, a deeper knowledge of the performance of

26   airborne microorganisms would allow improving the designs of the air-conditioning

27   installations to restrict hospital-acquired infections (HAIs). A solution containing

28   *Escherichia coli* (*E. coli*) as a model of airborne bacteria was nebulized using the Collison

29   nebulizer to simulate bioaerosols in various hospital areas such as patients' rooms or

30   bathrooms. Results showed that the bioaerosol source had a significant influence on the

31   airborne bacteria concentrations since $4.00 \ 10^2$, $6.84 \ 10^3$ and $1.39 \ 10^4$ $CFU \ mL^{-1}$ were

32   monitored during the aerosolization for 10 min of urine, saliva and urban wastewater,

33   respectively. These results may be explained considering the quite narrow distribution

34   profile of drop sizes around 1.10 - 1.29 μm obtained for urban wastewater, with much

35   vaster distribution profiles during the aerosolization of urine or saliva. The airborne

36   bacteria concentration may increase up to 10^7 $CFU \ mL^{-1}$ for longer sampling times and

37   higher aerosolization pressures, causing several cell damages. The cell membrane damage

38   index (I_D) can vary from 0 to 1, depending on the genomic DNA releases from bacteria.

39   In fact, the I_D of *E. coli* was more than two times higher (0.33 *vs.* 0.72) when increasing

40   the pressure of air flow was applied from 1 to 2 bar. Finally, the ventilation air flow also

41   affected the distribution of bioaerosols due to its direct relationship with the relative

42   humidity of indoor air. Specifically, the airborne bacteria concentration diminished

43   almost below 3-logs by applying more than 10 $L \ min^{-1}$ during the aerosolization of urine

44   due to their inactivation by an increase in their osmotic pressure.

45   **Keywords:** bioaerosol; hospital; saliva; urban wastewater; urine

1. Introduction

In recent years, the COVID-19 pandemic caused by the SARS-CoV-2 virus has aroused the scientific interest in infectious organisms which are transmitted via the airborne route (Ma et al., 2021). Not only viruses but also fungi and bacteria may be considered airborne infectious organisms. In fact, more than one million people die each year caused by fungal infections such as *Candida*, *Cryptococcus* and *Aspergillus* (Janbon et al., 2019). Likewise, bacteria such as *Streptococcus pyogenes*, *Corynebacterium diphtheriae*, *Klebsiella pneumoniae*, *E. coli*, *Neisseria meningitidis*, *Mycobacterium tuberculosis*, *Legionella pneumophila* may cause scarlet fever, diphtheria, classical pneumonia, urinary tract infection, meningitis, tuberculosis or legionellosis, respectively (Kim et al., 2018). The airborne biological particles which are comprised of fungal spores, bacterial cells, viruses, pollen grains, etc. may be defined as bioaerosols (Roca-Barcelo et al., 2020; Stetzenbach, 2009; Zia et al., 2021).

Potentially pathogenic bioaerosols may lead to hospital-acquired infections (HAIs), above all in hospital areas with natural ventilation where the bioaerosol concentrations are around 201 CFU/m^3 (Stockwell et al., 2019). It is estimated that 20 % of HAIs are caused by contact of patients with airborne pathogens since the average person inhales approximately 10 m^3 of air per day (Hopman et al., 2019; López-Cerero, 2014; Montagna et al., 2016; Weinstein, 1991). In this regard, humans produce more than 100, 1,000 and 100,000 particles as a consequence of the atomization of saliva and mucus in the oral cavity due to shearing from breathing when talking, coughing and sneezing, respectively (Xie et al., 2018). Additionally, liquid bioaerosols are also released during human hygiene practices such as showering, operating taps or toilet flushing as consequence of the biofilm growth on appliances and microbes present in wastewater as urine (Alsved et al., 2020). Kizny Gordon et al. reported that wastewater was a source of transmission of

71 carbapenemase-producing Enterobacteriaceae in intensive care units (Kizny Gordon et

72 al., 2017). Likewise, the removal of sinks from rooms also resulted in a decrease in

73 infections with multidrug-resistant microorganisms in intensive care units (Hopman et

74 al., 2017; Mathers et al., 2018).

75 The capability of bacteria to survive and maintain their pathogenicity in the ambient air

76 depends on the following atmospheric conditions: relative humidity, temperature or

77 chemical composition (Lin and Marr, 2020). Indeed, the experimental aerosolization of

78 microorganisms inside atmospheric simulation chambers is influenced by aerosol

79 generation, injection, residence time or sampling (Alsved et al., 2020). The performance

80 of aerosol generators has not been widely studied since there is still a lack of information

81 about their availability to provide high particle concentrations while enhancing the

82 preservation of cultivability and structural integrity of the aerosolized microorganisms

83 (Zhen et al., 2014). The liquid atomization may be developed by twin-fluid atomization

84 (Collison nebulizer, Sparging Liquid Aerosol Generators (SLAG), Pari LC Sprint, Flow

85 focusing Monodisperse Aerosol Generator (FMAG), etc.), centrifugal aerosolization

86 (Spinning Top Aerosol generators (STAG)), ultrasonic aerosolization (Sonotek™,

87 Omron microair, etc.), vibrating mesh aerosolization (Omron, Pari, etc.), electrospray

88 ionization or pulsed droplet ejection (Alsved et al., 2020; Danelli et al., 2021). The

89 Collison nebulizer is the most frequently used bioaerosol generator due to its high

90 reproducibility and its widespread application which allows it to compare with other

91 studies (Hart et al., 2020; Ibrahim et al., 2015). The Collison nebulizer is based on the

92 Bernouilli principle since a high velocity air flow passes through the nebulizer's small

93 orifice and, simultaneously, it suctions the liquid contained in the nebulizer's jar to

94 atomize the liquid (to break the liquid into small droplets) (May, 1973).

95   The airborne particles attach to any surface in contact due to adhesive forces as van der

96   Waals, electrostatic or surface tension. Thus, the air sampling methodologies depend on

97   various parameters as aerodynamic diameter or adhesion of airborne particles (Robotto

98   et al., 2021; Verreault et al., 2008). The aerodynamic diameters in the order 0.1-100 µm

99   allow bioaerosols to move in a particular way called Brownian motion (< 0.1 µm)

100   influenced by gravitational attraction (> 0.1 µm). The bioaerosol samplers may be filters,

101   electrostatic precipitators, liquid impactors (All-Glass Impinger (AGI), BioSampler, etc.)

102   or solid impactors (Andersen, slit or cyclone samplers). Among them, liquid impactors

103   accelerate particles through a narrow orifice located at a fixed distance from the bottom

104   of a flask and thus, particles enter through the inlet of the impinger due to a pressure drop

105   in the flask containing a liquid. These biosamplers present a great bioefficiency since they

106   are the least destructive samplers and also prevent the desiccation of airborne particles,

107   improving the extraction of genetic material for data analysis (Haig et al., 2016; Mainelis,

108   2020).

109   The composition and concentration of bioaerosols in hospital indoor air reported in the

110   literature, show the importance of further study in improving air quality to restrict HAIs.

111   In this context, quantitative estimations of airborne microorganisms would allow to

112   improve the designs of the air-conditioning systems for the cleanliness of the indoor air.

113   Then, the present study was also conducted to determine the influence of the bioaerosol

114   source and the ventilation air flow on the distribution of bioaerosols in indoor hospital

115   environments. The *E. coli* ATCC25922 was used as a model of airborne bacteria. The

116   Collison nebulizer was used to simulate bioaerosols in various hospital areas as patients'

117   rooms or bathrooms and then, sampled in a liquid solvent not only to be monitored but

118   also to quantify the cell damage of airborne bacteria.

119

2. Material and methods

2.1. Chemicals and bacterial strains

The chemicals used to prepare the simulated hospital aqueous solutions (urine, saliva, untreated urban wastewater) have been specified in the supplementary material.

Escherichia coli ATCC25922 provided from Scharlab, Spain, was used as a model of bacteria in this research. A sterile phosphate buffer solution (PBS) was used to collect bioaerosols and it was constituted of sodium chloride, potassium chloride, disodium phosphate dodecahydrate and potassium dihydrogen phosphate received from Sigma Aldrich.

2.2. Experimental procedure

Figure 1 shows the experimental setups to simulate bioaerosols in a hospital indoor air, coupled to a collection unit. Synthetic aqueous solutions with 10^8 CFU mL^{-1} of *E. coli* are nebulized through a pneumatic nebulizer namely Collison nebulizer with 3-jet (CH Technologies, USA) inside a PVC column with dimensions of 95 cm length and 11 cm diameter. Table 1 shows the chemical composition of the synthetic aqueous solutions that have been tested. An air compressor (JOSVAL SAUBER PORTABLE, Spain) is used to introduce dry air to the experimental devices, previously filtered using HEPA filters (Cytiva, Spain). The nebulized droplets are finally collected in a glass bubbler (Duran 45/40, Spain) which contains 60 mL of PBS. Additionally, the temperature and the relative humidity inside the PVC column are monitored with a thermo-hygrometer 810-195 (Gesa, Spain).
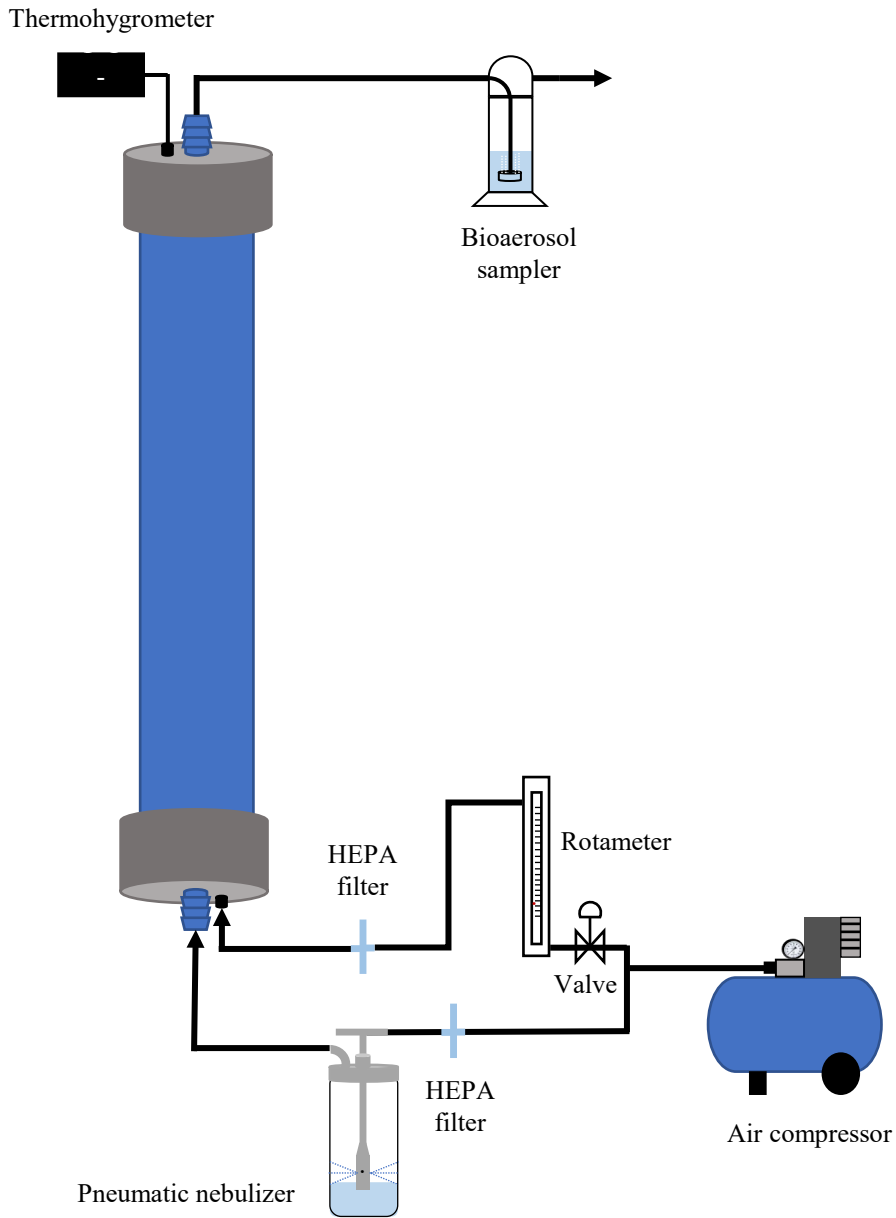
Table 1. Chemical composition of the synthetic aqueous solutions nebulize.

Aerosolized solutions	Chemicals	Concentration / mg L^{-1}	Ref.
Urine, pH$_{initial}$ = 5.98	CH_4N_2O	3333.34	(Herraiz-Carboné et al., 2020)
	$C_5H_4N_4O_3$	50	
	$C_4H_7N_3O$	166.67	
	KCl	1000	
	$MgSO_4$	170	
	$(Ca)_3(PO_4)_2$	28.34	
	Na_2CO_3	166.67	
	$(NH_4)_2HPO_4$	83.34	
Saliva, pH$_{initial}$ = 7.30	NaCl	9000	(Lakhloufi et al., 2020)
	KCl	400	
	$CaCl_2, H_2O$	200	
	$NaHCO_3$	200	
Untreated urban wastewater, pH$_{initial}$ = 7.00	$(NH_4)_2SO_4$	70	(Rawat et al., 2011)
	KH_2PO_4	20	
	$NaHCO_3$	100	
	$MgSO_4 \cdot 7H_2O$	10	
	$CaCl_2$	50	
	Glucose	1500	
	Peptone	1500	

142

143 Synthetic aqueous solutions were infected with *E. coli* ATCC25922 to simulate

144 bioaerosols in a hospital indoor air. The bacterial strains used were cultured at 37 °C for

145 24 h in Tryptone Soy Agar plates (Scharlab S.L., Spain) and later, resuspended into the

146 synthetic aqueous solutions up to an initial concentration of 10^8 CFU mL^{-1}.

147 All experiments were conducted in triplicate, and the results were expressed as the mean

148 values since the standard deviation in biological analyses was below 5 %.

Thermohygrometer

Bioaerosol
sampler

HEPA
filter

Rotameter

Valve

Air compressor

HEPA
filter

Pneumatic nebulizer

149

Figure 1. Experimental setup of aerosolization process with a pneumatic nebulizer. The air supplied by the compressor regulates the flow rate for dilution air using a rotameter whereas a manometer was used to control the pressure for the nebulizer. The bioaerosol and dilution air were mixed in the column. The bioaerosol was collected in the glass bubbler named bioaerosol sampler.

2.3. Aerosol particle number concentration

156   An optical particle sizer (OPS) TSI Model 3330 (TSI Inc., USA) based on light scattering,

157   coupled to a diffusion dryer 3062-NC (TSI Inc., USA) is used to measure the

158   concentration of aerosolization particles at 30 seconds resolution. The inlet air flow was

159   1 L min^{-1} and the results are mean values from 10 measurements carried out each 30

160   seconds, with a standard deviation below 5 %.

161   **2.4. Biological analyses**

162   A brief description of the biological analyses is developed in this section since the

163   analytical methods have been described elsewhere (Herraiz-Carboné et al., 2020; Zhen et

164   al., 2014). More detail information may be also found in the supplementary material.

165   **2.4.1. Analysis of *E. coli***

166   The concentration of *E. coli* was determined by an indirect impedance method using the

167   μ-Trac$^{®}$ 4200 system (SY-LAB, Austria).

168   **2.4.2. Analysis of 16S rRNA gene**

169   The analysis of 16S rRNA gene was developed as described in the literature by Zhen et

170   al. (Zhen et al., 2014). The 16S rRNA gene was previously extracted from samples and

171   then, it was quantified using a QuantStudio 5 Real-Time PCR System (Thermo Fischer

172   Scientific, Spain).

173   **2.4.3. Cell Membrane Damage Index**

174   The Cell Membrane Damage Index (I_D) was calculated following Equation (S1) (Zhen et

175   al., 2014).

176

3. Results and discussion

Table S1 summarizes a systematic review of the biological features in indoor bioaerosols within worldwide hospitals. A total of 34 journal articles were published related to airborne bacteria and fungi over the last five years. The most prevalent aerosolized bacteria were the genus *Staphylococcus* whereas the genus *Aspergillus* and *Penicillium* were the most frequent aerosolized fungi. The World Health Organization (WHO) recommends relatively relaxed limits of 100 CFU/m^3 for bacteria and 50 CFU/m^3 for fungi in the indoor air of hospitals (World Health Organization. Regional Office for, 1990). Nevertheless, the bioaerosol concentrations vary among hospital areas from 10^1 – 10^3 CFU/m^3 in inpatient facilities including bathrooms and 10^1 CFU/m^3 within intensive care units. These results are directly related to patients, building materials, air conditioning systems, ventilation types and other sources that generate, concentrate, or disperse bioaerosols in enclosed spaces.

The qualitative and quantitative estimations of airborne microorganisms are quite significant from the point of view of improving the designs of the thermal installations in hospitals for the cleanliness of the indoor air that is concerning human health. Therefore, the present study was conducted to determine the influence of the bioaerosol source, attending not only the aerosolized aqueous solutions but also how they are aerosolized, and the ventilation air flow on the distribution of bioaerosols in indoor hospital environments. Firstly, synthetic solutions of urine, saliva and urban wastewater spiked with 10^8 CFU mL^{-1} of *E. coli* (ATCC 25922) were aerosolized to simulate the indoor hospital air in various zones as patients' bathrooms during the flushing of a toilet, patients' rooms or other hospital areas (Douwes et al., 2003; Hopman et al., 2019; Lou et al., 2021). Figure 2 shows the total airborne bacteria concentration that was sampled in a sterile phosphate buffer (150 mM, pH 7.2) after 10 min of aerosolization of these

10

202   synthetic solutions, using the Collison nebulizer under 1 bar of the pressure of air flow

203   applied.

204
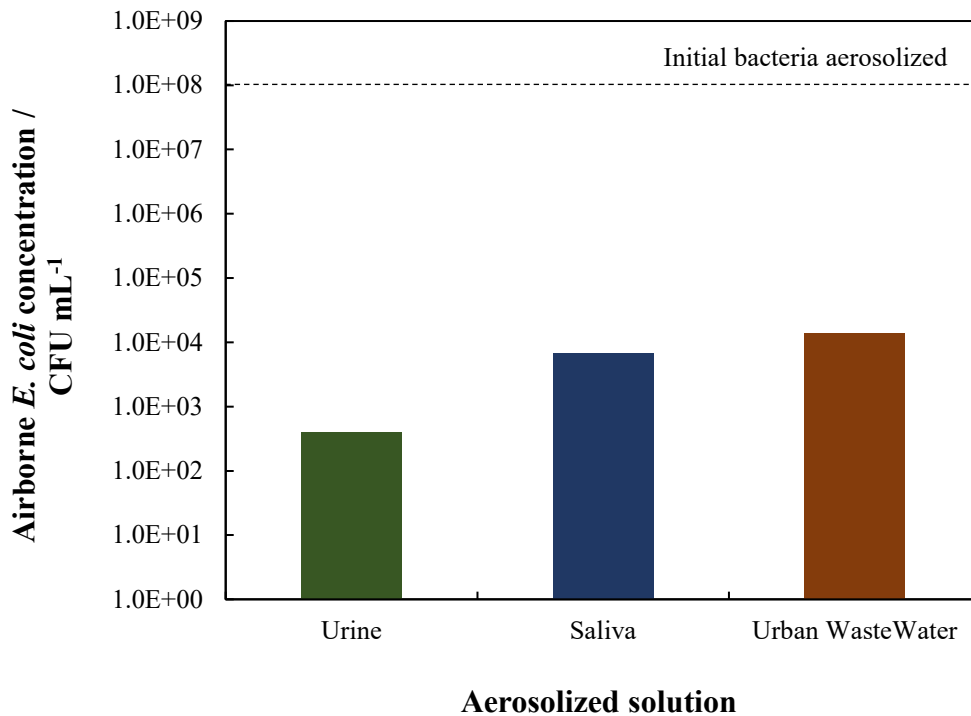
Figure 2. Total airborne *E. coli* concentration collected in a liquid solvent as a function

of the aerosolized solution of synthetic urine, saliva or urban wastewater contained 10^8

CFU mL^{-1} using the Collison nebulizer. The pressure of aerosolization air flow applied

through the Collison nebulizer: 1 bar. Sample collection: 10 min.

209   The aerosolized aqueous solutions are observed to significantly influence the bacteria

210   concentrations in the simulated indoor air. Specifically, the airborne bacteria

211   concentration increases in the following order: urine ($4.00 \cdot 10^2$ CFU mL^{-1}) < saliva (6.84

212   10^3 CFU mL^{-1}) < urban wastewater ($1.39 \cdot 10^4$ CFU mL^{-1}) for an experimental time of 10

213   min. This fact means that the aerosolization of urban wastewater promotes a faster

214   production of airborne bacteria, despite the same initial concentration of bacteria being

215   spiked in each solution (10^8 CFU mL^{-1} of *E. coli*). Herein, aerosol physics may explain it

216   since the settling velocity of aerosol particles depends on particles sizes, e.g. aerosol

11

217   particles of 0.2, 0.5, 1, 2, 5, 10 and 20 µm with a density of 1 g/cm^3 in room air at 20 ºC

218   present settling velocities of 1.2, 7.5, 30, 119, 746, 2 985 and 11 942 µm/second,

219   respectively (Scheuch, 2020). To shed light on the influence of the aerosolized aqueous

220   solutions on the airborne bacteria concentrations, Figure 3 shows the distribution of

221   aerosolized particles during the aerosolization of urine (Figure 3a), saliva (Figure 3b) and

222   urban wastewater (Figure 3c). An optical particle sizer was used to measure aerosolized

223   particles in 16 user adjustable size channels. The particle size distribution was selected in

224   the size channels from 0.7 to higher than 9.26 µm (random selection).

225
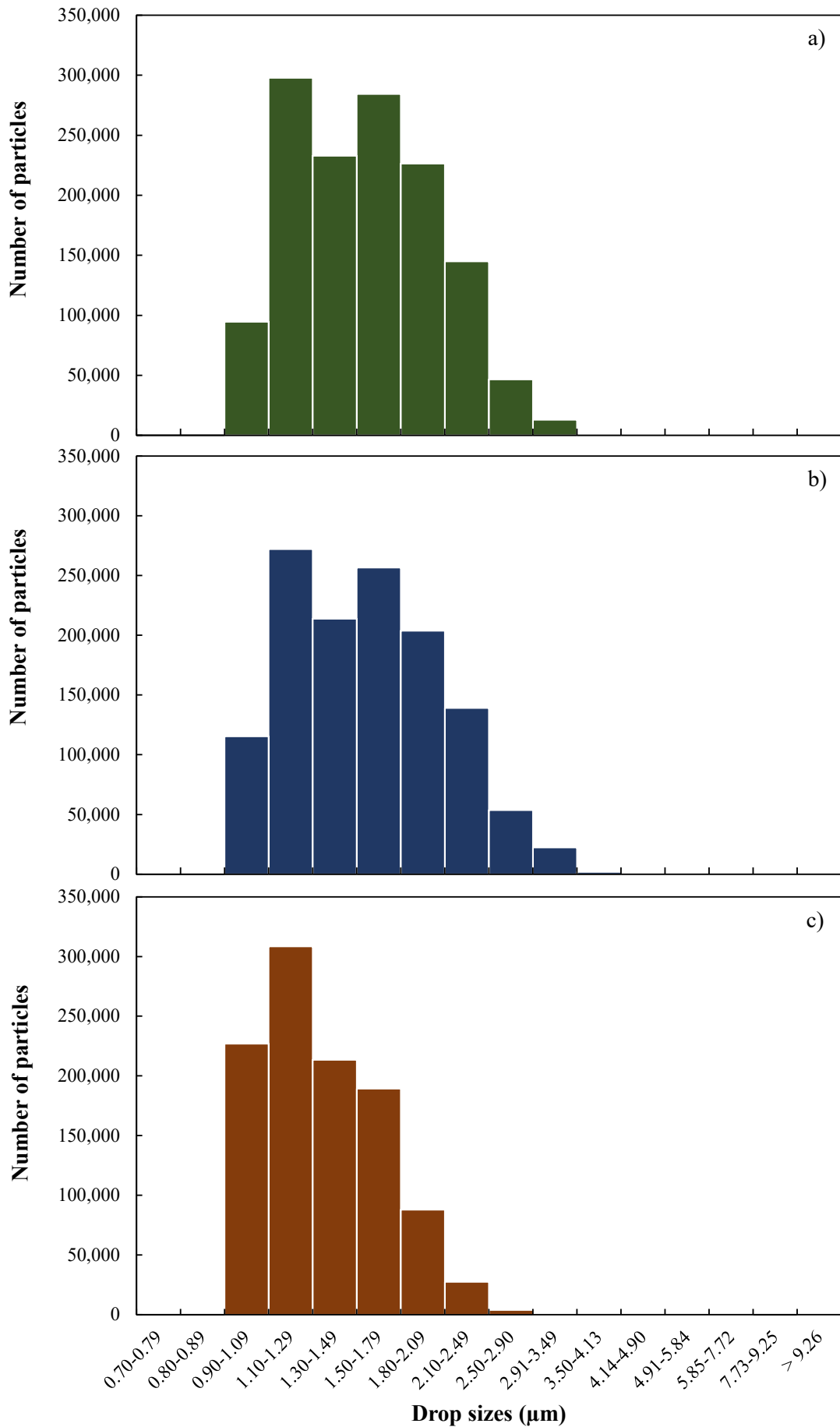
Figure 3. Distribution profiles of aerosolized particles, during the aerosolization of synthetic urine (a), saliva (b) and urban wastewater (c) within an initial concentration of 10^8 CFU mL^{-1} of *E. coli*.

As can be observed, the aerosolized droplets follow a log-normal distribution. However, the distribution profile depends on the chemical composition of the nebulized solution. In fact, the highest peak particle concentration occurs at the drop size range from 1.10 to 1.29 μm. Specifically, 297 767, 271 950 and 308 351 particles are attained during aerosolization of urine, saliva and urban wastewater, respectively. Additionally, the aerosolization of urban wastewater leads to a quite narrow distribution profile of drop sizes around the main peak whereas it is observed a much vaster distribution profile during the aerosolization of urine or saliva. Specifically, 227 000 particles within the drop size range 0.90 - 1.09 μm are monitored during the aerosolization of urban wastewater meanwhile less than half of the particles are detected for the other nebulized solutions (115 368 for saliva, 94 461 for urine) at the same drop size range. Upper to a particle size of 1.30 μm, a quite similar distribution of aerosolized particles is observed for saliva and urine since their distribution percentages differ between 16.7 and 17.4 % at 1.30 - 1.49 μm, 20.1 and 21.2 % at 1.50 - 1.79 μm, 15.9 and 16.9 % at 1.80 - 2.09 μm, 10.9 and 10.8 % at 2.10 - 2.49 μm, 4.5 and 3.5 % at 2.50 - 2.90 μm, 1.7 and 1.0 % at 2.91 – 3.49 μm, respectively. In literature, it is reported that the surface tension of aqueous solutions presents a great impact on the size of the produced droplet from nebulizers. The surface tension depends on the chemical composition and the temperature of a liquid (Arzhavitina and Steckel, 2010; Steckel and Eskandar, 2003). As shown in Table 1, the chemical composition of the aerosolized liquids is quite different, and it may explain a decrease in the droplet size when aerosolizing urban wastewater. Similarly, Zhang et al. reported that the chemical composition of fog water was directly related to the droplet size since larger

14

252 droplets (≥ 22 μm) contained higher Ca^{+2} concentration from soil sources whereas smaller

253 droplets (4-16 μm) presented higher NO_3^- and NH_4^+ concentrations due to industrial

254 sources and vehicles (Zhang et al., 2021). Leena et al. found that the aerosol chemical

255 composition showed a higher sulphate and ammonium contribution during low aerosol

256 loading days in Western Ghats (India) (Leena et al., 2022). Likewise, Ivanov et al. studied

257 the influence of various chemical components on the size distribution of artificially

258 generated fog droplets. Higher mean particle size was observed when increasing the

259 concentration of potassium dihydrogen phosphate compared to pure water fog (Ivanov et

260 al., 2020). In this context, the formation of a large number of aerosolized particles with

261 smaller size may explain the highest airborne *E. coli* concentration observed in Figure 2

262 from urban wastewater.

263 Herein, not only the aerosolized aqueous solutions but also how they are aerosolized may

264 influence the airborne bacteria concentrations. For instance, human mouths may be

265 considered nebulizers that produce about 100 particles when speaking, 1000 particles

266 when coughing and more than 100 000 particles when sneezing (Xie et al., 2018).

267 Synthetic solutions of urine, saliva and urban wastewater spiked with 10^8 CFU mL^{-1} of

268 *E. coli* (ATCC 25922) were aerosolized under different pressures to simulate the indoor

269 hospital air. Figure 4 depicts the influence of the pressure of air flow applied through the

270 Collison nebulizer from 1 to 3 bar on the airborne *E. coli* concentration that was

271 monitored after the collection in the liquid solvent at two different times (10 and 180

272 min).
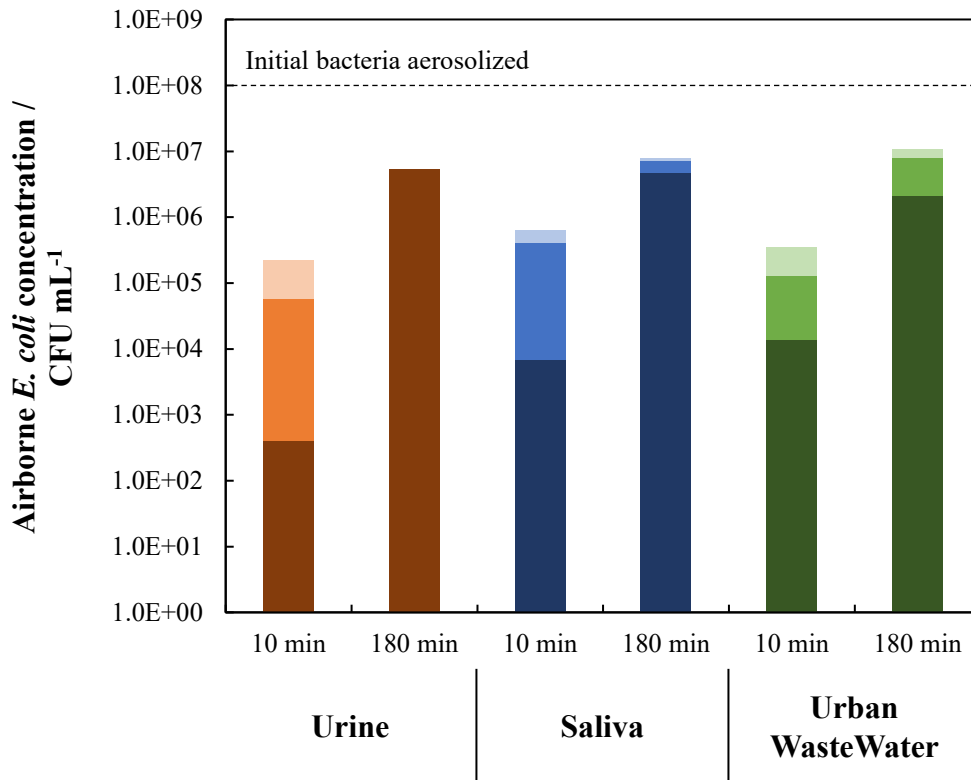
Figure 4. Total airborne *E. coli* concentration collected in a liquid solvent as a function of the solution nebulized, during the aerosolization of synthetic urine, saliva or urban wastewater contained 10^8 CFU mL^{-1} of *E. coli*. The pressure of aerosolization air flow applied through the Collison nebulizer: (dark-colored bars) 1 bar, (medium-colored bars) 2 bar, (light-colored bars) 3 bar.

As can be observed, the higher the pressure of aerosolization air flow applied through the Collison nebulizer, the higher the airborne *E. coli* concentration for each nebulized solution tested. Within the first 10 min, the airborne *E. coli* concentration increases up to almost 2-logs when inlet air pressure increases 1 bar (from 1 to 2 bar) and even up to almost 3-logs with an increment of 2 bar (from 1 to 3 bar). Specifically, the airborne *E. coli* concentration is $4 \cdot 10^2$ CFU mL^{-1} with an applied air pressure of 1 bar, $5.79 \cdot 10^4$ CFU mL^{-1} for 2 bar and $1.64 \cdot 10^5$ CFU mL^{-1} for 3 bar, during the first 10 min of aerosolization of urine. Conversely, a negligible influence of the pressure of aerosolization air flow may be considered at 180 min since the airborne *E. coli* concentration is increased by less than

288   1-log. Here, it is important to highlight that the experimental device (Figure 1) operates

289   in continuous mode and then, the stationary state is attained after 120 min (data not

290   shown). Once reached the stationary state, the airborne *E. coli* concentration is not

291   influenced by the chemical composition of the aerosolized solution. To shed light on how

292   the pressure of aerosolization air flow applied may influence the airborne bacteria

293   concentration, Figure 5 shows the distribution profiles of bioaerosol particles during the

294   aerosolization of urine (Figure 5a), saliva (Figure 5b) or urban wastewater (Figure 5c).

Number of particles (y-axis, all panels: 0 – 400,000)

Drop sizes / μm

a)

b)

c)
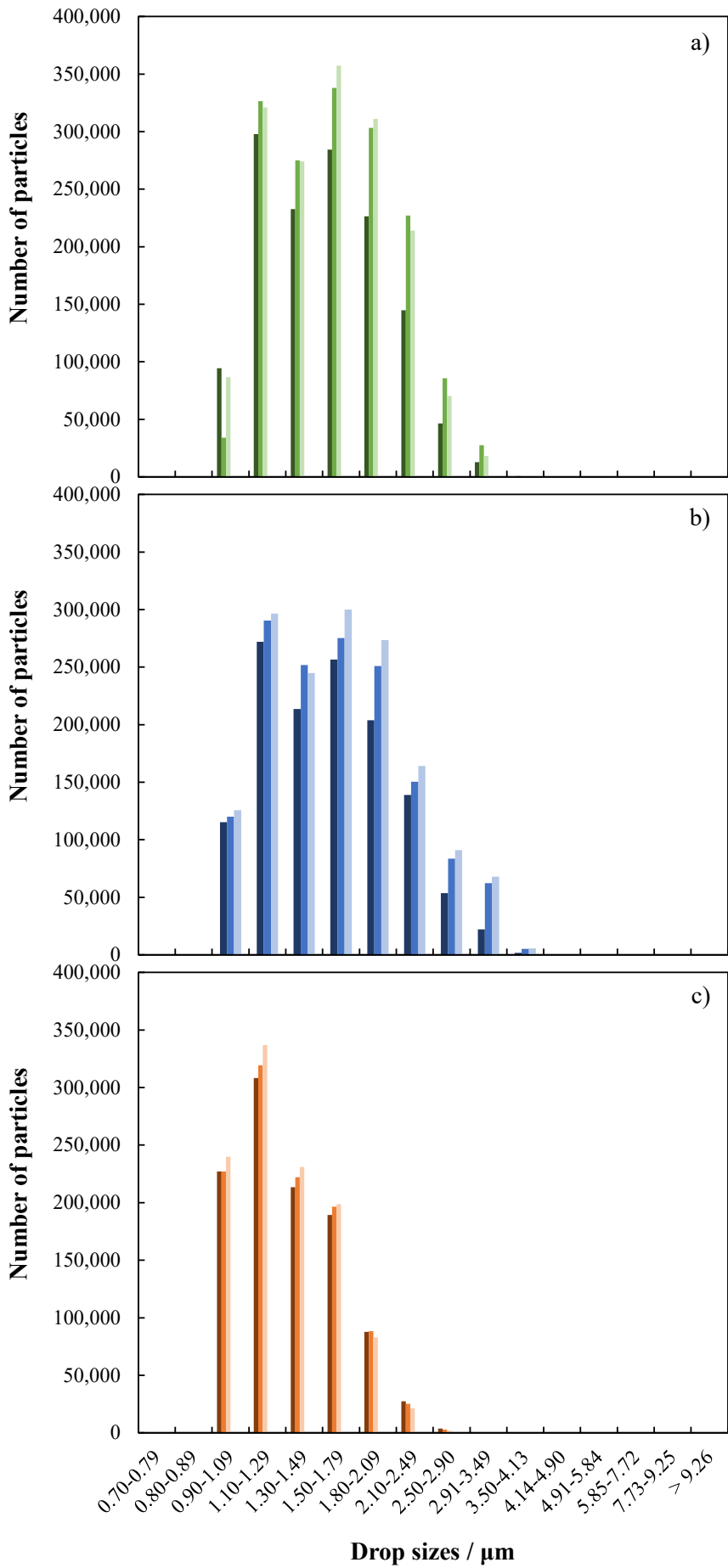
296   **Figure 5.** Distribution profiles of bacteria airborne particles, during the aerosolization of

297   synthetic urine, saliva or urban wastewater contained 10^8 CFU mL^{-1} of *E. coli*. The

298   pressure of aerosolization air flow applied through the Collison nebulizer: (dark-colored

299   bars) 1 bar, (medium-colored bars) 2 bar, (light-colored bars) 3 bar.

300   As can be observed, the distribution profiles of particle sizes are similar to those explained

301   in Figure 3. As previously, 20 – 30 % of the total aerosolized particles have a size in the

302   range of 1.10 – 1.29 μm. Nevertheless, a larger number of particles are aerosolized when

303   increasing the pressure of air flow applied through the Collison nebulizer, regardless the

304   solution being nebulized. This increment is the most significant when nebulizing urine

305   since the number of total aerosolized particles increases up to 20.7 and 23.3 % when

306   applying air pressures of 2 and 3 bar, respectively. Conversely, the total number of

307   particles only increases up to 2.3 and 5.2 % during the aerosolization of urban wastewater

308   at 2 and 3 bar, respectively. This fact may explain the influence of the aerosol outlet on

309   the airborne *E. coli* concentration for the different nebulized solutions in Figure 4. The

310   higher the increase in the total number of particles, the higher the airborne *E. coli*

311   concentration since the distribution of particle sizes is the same, despite the pressure of

312   air flow applied.

313   In literature, the membrane of *E. coli* and *Bacillus atrophaeus* bacteria has been reported

314   to suffer impairment due to the stress experienced by bacteria due to aerosolization and

315   air sampling. As consequence, DNA is released as free molecules and the damage may

316   be quantified by calculating the cell membrane damage index (I_D) as shown in Equation

317   1 (May, 1973; Zhen et al., 2013). Figure 6 presents the I_D for *E. coli* aerosolized by the

318   Collison nebulizer till reach the steady state in the experimental device (180 min) at

319   pressures of 1, 2 and 3 bar of air flow applied. At each tested pressure, the plotted I_D value

320   is the arithmetic mean among the I_D values obtained for each nebulized solutions (urine,

321 saliva, urban wastewater). It is noticeable that I_D varies from 0 (no membrane damage of

322 bacterial cells) to 1 (all genomic DNA from bacteria has been released and it has been

323 measured as the amount of 16S rRNA genes released).

324
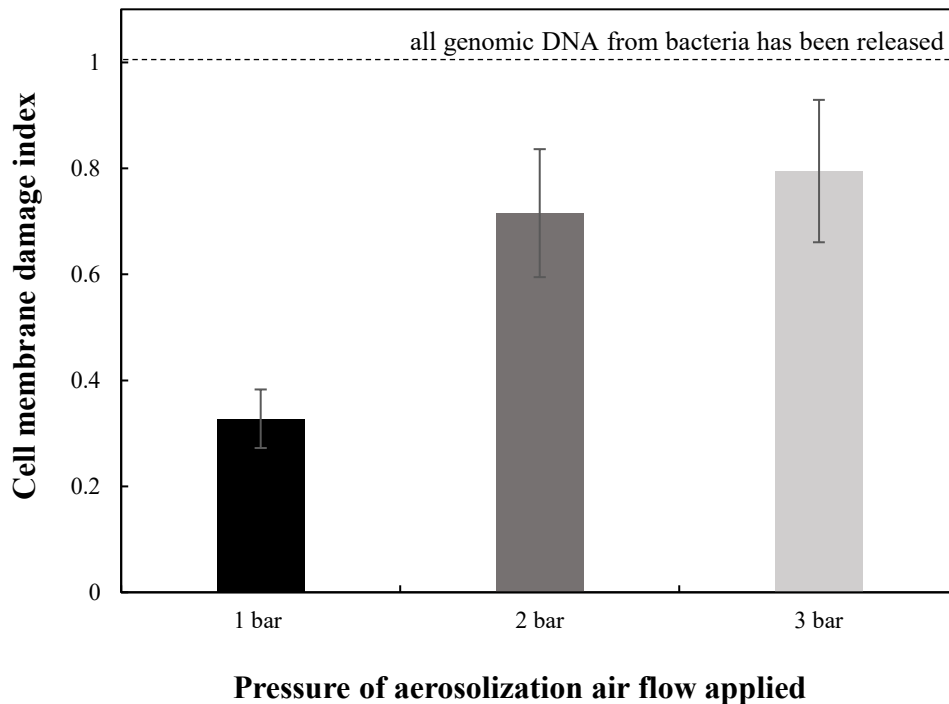
Figure 6. Cell membrane damage index (I_D) of *E. coli* bacteria aerosolized under different

326 pressures of air flow applied through the Collison nebulizer during 180 min. Bars are

327 averages of I_D values obtained during the aerosolization of urine, saliva and urban

328 wastewater spiked with 10^8 CFU mL^{-1} of *E. coli*.

329 As can be observed, a significant difference in I_D is found as a function of the

330 aerosolization pressures. The membrane damage of bacterial cells is higher when

331 increasing the pressure of air flow applied. The I_D values are 0.33, 0.72 and 0.80 with a

332 16.9 % of error for aerosolization pressures of 1, 2 and 3 bars, respectively. The I_D value

333 increases up to two-folds from 1 bar to 2 bar, although it increases less than 0.10 units

334 from 2 to 3 bar. This means that the cell membrane damage does not proportionally

335 depend on the increment of the pressure of air flow applied. Indeed, Zhen et al. found an

336   I_D value of around 0.11 for 15 psi and 0.36 for 40 psi when nebulizing sterile deionized

337   water with 10^9 CFU mL^{-1} of *E. coli,* using the Collison nebulizer and sampling in a

338   BioSampler for 5 min (Zhen et al., 2013).

339   Finally, the distribution of bioaerosols in indoor hospital environments may be changed

340   by the ventilation air flow. The ventilation is a tool to maintain safe and healthy conditions

341   by reducing or eliminating environmental pollutants generated in enclosed places. If the

342   ventilation air is also air-conditioned, it allows being in comfortable conditions. Figure 7

343   shows the influence of the ventilation air flow (0 – 15 L min^{-1}) as a function of the

344   nebulized solution (urine, saliva, urban wastewater). The performance of the ventilation

345   air flow is mainly focused on the airborne *E. coli* concentration and on the relative

346   humidity attained under the steady state operation mode (180 min).

347
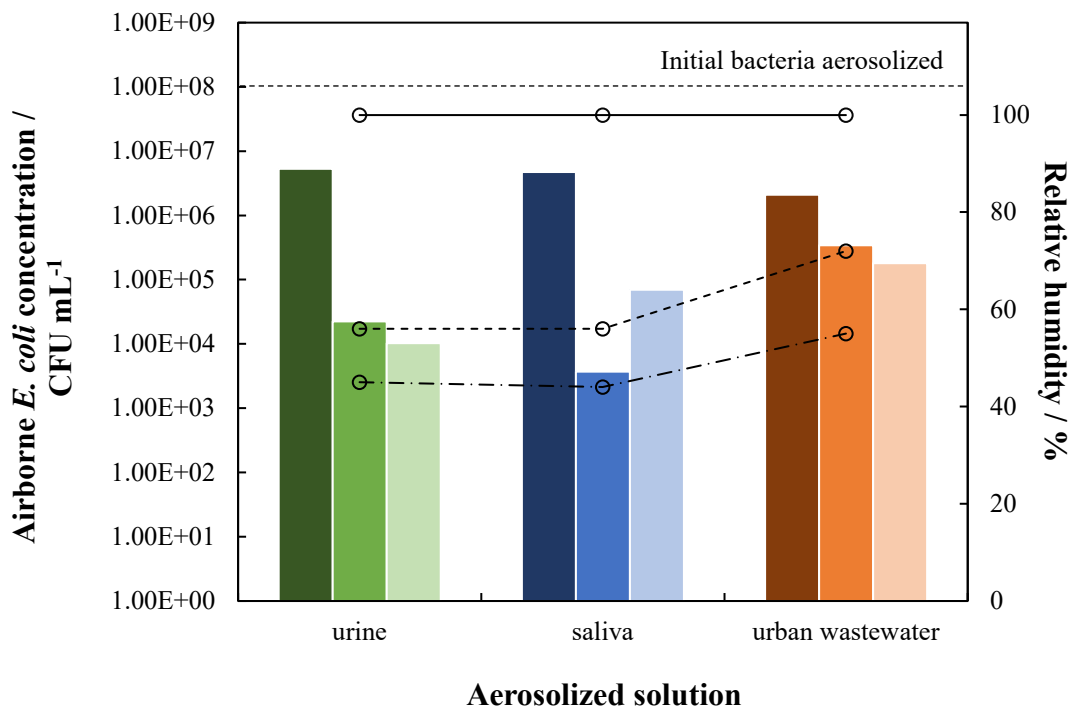
348   **Figure 7.** Total airborne *E. coli* concentration (bars) and relative humidity (points) as a

349   function of the solution nebulized during the aerosolization of synthetic urine, saliva or

350   urban wastewater contained 10^8 CFU mL^{-1} for 180 min. The pressure of aerosolization

351   air flow applied through the Collison nebulizer: 1 bar. Ventilation air flow: (dark-colored

352   bars) 0 L min^{-1}, (medium-colored bars) 10 L min^{-1}, (light-colored bars) 15 L min^{-1}.

353   In general, it is observed that the higher the ventilation air flow the lower the airborne *E.*

354   *coli* concentration. The aerosolization of urine leads to a more significant influence on

355   the ventilation air flow since the concentration of airborne *E. coli* diminishes almost

356   below 3-logs by applying more than 10 L min^{-1}. This performance is much less significant

357   when urban wastewater is aerosolized with less than 1-log of bacteria concentration

358   reduction. The influence of the ventilation air flow on the airborne *E. coli* concentration

359   seems to be directly related to the relative humidity monitored inside the test chamber at

360   each test. Specifically, the highest airborne *E. coli* concentration is observed at 100 % of

361   relative humidity without any ventilation air flow despite the aerosolized solution tested.

362   Additionally, the higher the ventilation air flow the lower the percentage of relative

363   humidity monitored and then, the lower concentration of *E. coli* monitored. For instance,

364   the airborne *E. coli* concentration varies among 2.09 10^6, 3.41 10^5 and 1.81 10^5 CFU mL$^-$

365   ^{1} with a 100, 72 and 55 % of relative humidity under the aerosolization of urban

366   wastewater, using ventilation air flows of 0, 10 and 15 L min^{-1}, respectively. This may be

367   explained bearing in mind that microorganisms may survive better in an environment

368   with high relative humidity since it is known that they stop growing when their growth

369   medium dries out. A low relative humidity leads to an increase the concentrations of salts

370   as droplets evaporate and then, the osmotic pressure of bacteria increases resulting in their

371   inactivation (Lin and Marr, 2020; Wang et al., 2001). In literature, the greatest survival

372   of aerosolized Gram-negative bacteria (including *Pseudomonas*, *Enterobacter* and

373   *Klebsiella species*) was found to take place in high relative humidity (Marthi et al., 1990;

374   Tang, 2009; Walter et al., 1990). Likewise, Theunissen et al. observed an optimal survival

375　of *Chlamydia pneumoniae* in aerosols at a 95 % of relative humidity (Theunissen et al.,

376　1993).

377

378　**4. Conclusions**

379　This work studies the influence of various parameters on the formation of airborne

380　microorganisms that have allowed to optimize the operation conditions that make

381　possible the physical simulation of hospital indoor air under a laboratory scale. It will

382　allow a future improvement of the designs of the air-conditioning installations or even an

383　enhancement of the methodologies of air treatment in hospitals. Within this framework,

384　the following conclusions can be drawn:

385　　● The bioaerosol source significantly affects the airborne bacteria concentrations

386　　　since the distribution of droplets is affected by the chemical composition of the

387　　　aerosolized solutions. Specifically, $4.00 \ 10^2$ CFU mL^{-1} of airborne *E. coli* are

388　　　monitored during aerosolization of urine, $6.84 \ 10^3$ CFU mL^{-1} with saliva and 1.39

389　　　10^4 CFU mL^{-1} from urban wastewater after sampling the first 10 min. Likewise,

390　　　the pressure of air flow applied during aerosolization also causes damage to

391　　　airborne microorganisms. This damage was measured considering that the cell

392　　　membrane damage index (I_D) can vary from 0 to 1, depending on the genomic

393　　　DNA releases from bacteria. Results show that the I_D of *E. coli* is more than two

394　　　times higher (0.33 *vs.* 0.72) when increasing the pressure of air flow applied from

395　　　1 to 2 bar.

396　　● The ventilation air flow also affects the distribution of bioaerosols in indoor

397　　　hospital environments. Specifically, the concentration of airborne *E. coli*

398　　　diminishes almost below 3-logs by applying more than 10 L min^{-1} during the

23

399   aerosolization of urine. Additionally, the ventilation air flow is directly related to

400   the relative humidity since the higher the ventilation air flow, the lower the

401   percentage of relative humidity monitored. This fact may explain a lower survival

402   of microorganisms under low relative humidity since it leads to an increase in the

403   concentrations of salts as droplets evaporate and then, the osmotic pressure of

404   bacteria increases resulting in their inactivation.

405

411

412   **References**

413   Alsved, M., et al., 2020. Natural sources and experimental generation of bioaerosols:

414   Challenges and perspectives. Aerosol Science and Technology. 54**,** 547-571.

415   Arzhavitina, A., Steckel, H., 2010. Surface active drugs significantly alter the drug output

416   rate from medical nebulizers. Int J Pharm. 384**,** 128-36.

417   Danelli, S. G., et al., 2021. Comparative characterization of the performance of bio-

418   aerosol nebulizers in connection with atmospheric simulation chambers. Atmos.

419   Meas. Tech. 14**,** 4461-4470.

420   Douwes, J., et al., 2003. Bioaerosol health effects and exposure assessment: progress and

421   prospects. Ann Occup Hyg. 47**,** 187-200.

422   Haig, C. W., et al., 2016. Bioaerosol sampling: sampling mechanisms, bioefficiency and

423   field studies. Journal of Hospital Infection. 93**,** 242-255.

424   Hart, M. B., et al., 2020. Toward biological aerosol reference standards. Aerosol Science

425   and Technology. 54**,** 601-610.

426   Herraiz-Carboné, M., et al., 2020. Removal of antibiotic resistant bacteria by electrolysis

427   with diamond anodes: A pretreatment or a tertiary treatment? Journal of Water

428   Process Engineering. 38.

429   Hopman, J., et al., 2019. Risk assessment after a severe hospital-acquired infection

430   associated with Carbapenemase-producing Pseudomonas aeruginosa. JAMA

431   network open. 2**,** e187665-e187665.

432   Hopman, J., et al., 2017. Reduced rate of intensive care unit acquired gram-negative

433   bacilli after removal of sinks and introduction of 'water-free' patient care.

434   Antimicrobial resistance and infection control. 6**,** 59-59.

435   Ibrahim, E., et al., 2015. An experimental investigation of the performance of a Collison

436   nebulizer generating H1N1 influenza aerosols. Biotechnology &

437   Biotechnological Equipment. 29**,** 1142-1148.

438   Ivanov, O., et al., 2020. Investigations on the Influence of Chemical Compounds on Fog

439   Microphysical Parameters. Atmosphere. 11**,** 225.

440   Janbon, G., et al., 2019. Studying fungal pathogens of humans and fungal infections:

441   fungal diversity and diversity of approaches. Microbes and Infection. 21**,** 237-245.

442   Kim, K.-H., et al., 2018. Airborne bioaerosols and their impact on human health. Journal

443   of Environmental Sciences. 67**,** 23-35.

444   Kizny Gordon, A. E., et al., 2017. The Hospital Water Environment as a Reservoir for

445   Carbapenem-Resistant Organisms Causing Hospital-Acquired Infections-A

446   Systematic Review of the Literature. Clinical infectious diseases : an official

447   publication of the Infectious Diseases Society of America. 64**,** 1435-1444.

448   Lakhloufi, S., et al., 2020. Electrochemical behavior and surface characterization of

449   dental materials in artificial salivary. Materials Today: Proceedings. 31**,** S141-

450   S148.

451   Leena, P. P., et al., 2022. Influence of aerosol physico-chemical properties on cloud

452   microphysical parameters perceived using in-situ high altitude observations.

453   Atmospheric Research. 271**,** 106111.

454   Lin, K., Marr, L. C., 2020. Humidity-Dependent Decay of Viruses, but Not Bacteria, in

455   Aerosols and Droplets Follows Disinfection Kinetics. Environmental Science &

456   Technology. 54**,** 1024-1032.

457   López-Cerero, L., 2014. Role of the hospital environment and equipment in the

458   transmission of nosocomial infections. Enfermedades Infecciosas y

459   Microbiologia Clinica. 32**,** 459-464.

460   Lou, M., et al., 2021. The bioaerosols emitted from toilet and wastewater treatment plant:

461   a literature review. Environmental Science and Pollution Research. 28**,** 2509-

462   2521.

463   Ma, J., et al., 2021. Coronavirus Disease 2019 Patients in Earlier Stages Exhaled Millions

464   of Severe Acute Respiratory Syndrome Coronavirus 2 Per Hour. Clinical

465   Infectious Diseases. 72**,** e652-e654.

466   Mainelis, G., 2020. Bioaerosol Sampling: Classical Approaches, Advances, and

467   Perspectives. Aerosol Sci Technol. 54**,** 496-519.

468   Marthi, B., et al., 1990. Survival of bacteria during aerosolization. Applied and

469   environmental microbiology. 56**,** 3463-3467.

470   Mathers, A. J., et al., 2018. Intensive Care Unit Wastewater Interventions to Prevent

471   Transmission of Multispecies Klebsiella pneumoniae Carbapenemase-Producing

472   Organisms. Clin Infect Dis. 67, 171-178.

473   May, K. R., 1973. The collison nebulizer: Description, performance and application.

474   Journal of Aerosol Science. 4, 235-243.

475   Montagna, M. T., et al., 2016. Serological and molecular identification of Legionella spp.

476   isolated from water and surrounding air samples in Italian healthcare facilities.

477   Environmental Research. 146, 47-50.

478   Rawat, I., et al., 2011. Dual role of microalgae: Phycoremediation of domestic wastewater

479   and biomass production for sustainable biofuels production. Applied Energy. 88,

480   3411-3424.

481   Robotto, A., et al., 2021. SARS-CoV-2 airborne transmission: A validated sampling and

482   analytical method. Environmental Research. 200, 111783.

483   Roca-Barcelo, A., et al., 2020. Risk of respiratory hospital admission associated with

484   modelled concentrations of Aspergillus fumigatus from composting facilities in

485   England. Environmental Research. 183, 108949.

486   Scheuch, G., 2020. Breathing Is Enough: For the Spread of Influenza Virus and SARS-

487   CoV-2 by Breathing Only. J Aerosol Med Pulm Drug Deliv. 33, 230-234.

488   Steckel, H., Eskandar, F., 2003. Factors affecting aerosol performance during

489   nebulization with jet and ultrasonic nebulizers. Eur J Pharm Sci. 19, 443-55.

490   Stetzenbach, L. D., 2009. Airborne Infectious Microorganisms. Encyclopedia of

491   Microbiology. 175-182.

492   Stockwell, R. E., et al., 2019. Indoor hospital air and the impact of ventilation on

493   bioaerosols: a systematic review. J Hosp Infect. 103, 175-184.

494   Tang, J. W., 2009. The effect of environmental parameters on the survival of airborne

495   infectious agents. Journal of the Royal Society, Interface. 6 Suppl 6**,** S737-S746.

496   Theunissen, H. J., et al., 1993. Influence of temperature and relative humidity on the

497   survival of Chlamydia pneumoniae in aerosols. Appl Environ Microbiol. 59**,**

498   2589-93.

499   Verreault, D., et al., 2008. Methods for sampling of airborne viruses. Microbiology and

500   molecular biology reviews : MMBR. 72**,** 413-444.

501   Walter, M. V., et al., 1990. Effect of aerosolization on subsequent bacterial survival.

502   Applied and environmental microbiology. 56**,** 3468-3472.

503   Wang, Z., et al., 2001. Effect of sampling time and air humidity on the bioefficiency of

504   filter samplers for bioaerosol collection. Journal of Aerosol Science. 32**,** 661-674.

505   Weinstein, R. A., 1991. Epidemiology and control of nosocomial infections in adult

506   intensive care units. Am J Med. 91**,** 179s-184s.

507   World Health Organization. Regional Office for, E., 1990. Indoor air quality: biological

508   contaminants: report on a WHO meeting, Rautavaara, 29 August–2 September

509   1988. World Health Organization. Regional Office for Europe, Copenhagen.

510   Xie, Z., et al., 2018. Characteristics of ambient bioaerosols during haze episodes in China:

511   A review. Environmental Pollution. 243**,** 1930-1942.

512   Zhang, S., et al., 2021. Chemical characteristics of size-resolved fog water at an urban

513   site in Nanjing and the summit of Mt. Lu, East China. Atmospheric Environment.

514   263**,** 118667.

515   Zhen, H., et al., 2013. Release of free DNA by membrane-impaired bacterial aerosols due

516   to aerosolization and air sampling. Appl Environ Microbiol. 79**,** 7780-9.

517   Zhen, H., et al., 2014. A systematic comparison of four bioaerosol generators: Affect on

518   culturability and cell membrane integrity when aerosolizing Escherichia coli

519   bacteria. Journal of Aerosol Science. 70**,** 67-79.

520   Zia, H., et al., 2021. Engineering Solutions for Preventing Airborne Transmission in

521   Hospitals with Resource Limitation and Demand Surge. Indian J Crit Care Med.

522   25**,** 453-460.

523